Developmental Biology 404 (2015) 49–60

Contents lists available at ScienceDirect

Developmental Biology

journal homepage: www.elsevier.com/locate/developmentalbiology

Polo-like kinase 2 regulates angiogenic sprouting and blood vessel development

Hongbo Yang [a], Longhou Fang [a], Rui Zhan [a], Jeffrey M. Hegarty [a], Jie Ren [a], Tzung K. Hsiai [b,c], Joseph G. Gleeson [d], Yury I. Miller [a], JoAnn Trejo [e], Neil C. Chi [a,f,*]

[a] Department of Medicine, University of California, San Diego, La Jolla, CA 92093-0613J, USA
[b] Division of Cardiology, Department of Medicine, School of Medicine, University of California, Los Angeles, CA, USA
[c] Department of Bioengineering, School of Engineering & Applied Science, University of California, Los Angeles, CA, USA
[d] Neurogenetics Laboratory, Howard Hughes Medical Institute, Department of Neurosciences, University of California, San Diego, La Jolla, CA 92093, USA
[e] Department of Pharmacology, School of Medicine, University of California, San Diego, La Jolla, CA 92093, USA
[f] Institute of Genomic Medicine, University of California, San Diego, La Jolla, CA 92093, USA

ARTICLE INFO

Article history:
Received 27 November 2014
Received in revised form
11 April 2015
Accepted 12 May 2015
Available online 22 May 2015

Keywords:
Polo-like kinase 2
Angiogenesis
Vascular development
Zebrafish
Human umbilical vein endothelial cells

ABSTRACT

Angiogenesis relies on specialized endothelial tip cells to extend toward guidance cues in order to direct growing blood vessels. Although many of the signaling pathways that control this directional endothelial sprouting are well known, the specific cellular mechanisms that mediate this process remain to be fully elucidated. Here, we show that Polo-like kinase 2 (PLK2) regulates Rap1 activity to guide endothelial tip cell lamellipodia formation and subsequent angiogenic sprouting. Using a combination of high-resolution *in vivo* imaging of zebrafish vascular development and a human umbilical vein endothelial cell (HUVEC) *in vitro* cell culture system, we observed that loss of *PLK2* function resulted in a reduction in endothelial cell sprouting and migration, whereas overexpression of *PLK2* promoted angiogenesis. Furthermore, we discovered that PLK2 may control angiogenic sprouting by binding to PDZ-GEF to regulate RAP1 activity during endothelial cell lamellipodia formation and extracellular matrix attachment. Consistent with these findings, constitutively active RAP1 could rescue the endothelial cell sprouting defects observed in zebrafish and HUVEC *PLK2* knockdowns. Overall, these findings reveal a conserved PLK2-RAP1 pathway that is crucial to regulate endothelial tip cell behavior in order to ensure proper vascular development and patterning in vertebrates.

Introduction

Angiogenesis is a highly integrative and reiterative cellular process involving the migration and proliferation of endothelial cells (EC) to form new blood vessels from pre-existing ones. It is dependent on the specification of specialized EC subtypes (Adams and Alitalo, 2007; De Smet et al., 2009; Lamalice et al., 2007) that play distinct roles in angiogenic sprouting. To this end, endothelial tip cells can extend filopodia- and lamellipodia-like processes to sense growth factors, extracellular matrix (ECM) components and attractive/repulsive cues that direct EC sprouting and migration (Adams and Alitalo, 2007; De Smet et al., 2009; Lamalice et al., 2007). In contrast, endothelial stalk cells, which reside behind the leading endothelial tip cells, proliferate to elongate the growing blood vessel. Recent studies have shown that Vascular endothelial growth factor (VEGF) and Notch signaling tightly control the differentiation of these EC subtypes (Gerhardt et al., 2003; Hellstrom et al., 2007; Roca and Adams, 2007; Siekmann and Lawson, 2007; Suchting et al., 2007). In particular, VEGF can induce tip cell specification and the expression of the Notch ligand Delta-like 4, which in turn activates Notch signaling in neighboring stalk cells to suppress VEGF receptor 2 expression and tip cell behavior. Furthermore, VEGF and other developmental signaling cues (Bedell et al., 2005; Herbert et al., 2009; Larrivee et al., 2009; Lee et al., 2002; Lu et al., 2004; Park et al., 2003; Torres-Vazquez et al., 2004; Weitzman et al., 2008) can also guide endothelial tip cell membrane extensions to control the proper development and patterning of the vascular network (Carmeliet and Tessier-Lavigne, 2005; Mukouyama et al., 2002; Zacchigna et al., 2008).

In order for ECs to directionally sprout and migrate to form the vasculature, a series of organized cellular events are required for endothelial tip cells to extend their membranes and migrate

* Corresponding author at: Department of Medicine, University of California, La Jolla, San Diego, CA 92093-0613J, USA.
E-mail address: nchi@ucsd.edu (N.C. Chi).

http://dx.doi.org/10.1016/j.ydbio.2015.05.011
0012-1606/

toward guidance cues. They initially extend multiple filopodia at their distal tips to sense guidance cues in their environment and subsequently form lamellipodia to create an EC leading edge that protrudes toward the chemotactic signal. These EC protrusions then attach to the ECM at focal adhesions to stabilize the sprouting EC membrane and prepare the endothelial tip cell for subsequent migration. A central cellular component in regulating many of these specific cellular events is the activation of small GTPases (Kiosses et al., 2001; Spindler et al., 2010; Wojciak-Stothard et al., 1998). In response to VEGF, Cdc42 promotes the growth of filopodia and mediates cell polarization through microtubule organization (Petrovic et al., 2007), whereas Rac1, together with PAK, controls lamellipodia generation (Kiosses et al., 1999, 2001; Somanath and Byzova, 2009). Moreover, RhoA/ROCK and Ras-associated protein 1 (Rap1) have also been discovered to regulate angiogenesis through the phosphorylation of focal adhesion kinase (FAK) as well as the activation of β1 and αVβ3 integrins (Carmona et al., 2009; Lakshmikanthan et al., 2011; van Nieuw Amerongen et al., 2003; Zeng et al., 2002). Consistent with these findings, both loss of function of Rap1 and PDZ-GEF, a guanine nucleotide exchange factor (GEF) for Rap1, results in vascular developmental defects in both mouse and zebrafish (Carmona et al., 2009; Chrzanowska-Wodnicka et al., 2008; Lakshmikanthan et al., 2011; Wei et al., 2007). Thus, specific small GTPases control distinct cellular events during EC sprouting and discovering the factors that regulate these small GTPases may provide insight as to how the activity of these small GTPases are coordinated to promote directional EC angiogenic sprouting and migration.

The polo-like kinase (PLK) family proteins have been previously shown to play pivotal roles in regulating the cell cycle (Simmons et al., 1992), including entry into mitosis, centrosome maturation, and exit from mitosis with the initiation of cytokinesis (Liu and Erikson, 2003). They contain two conserved domains – the canonical serine/threonine kinase domain and the non-catalytic polo box domain (PBD), which binds to substrates and targets the kinase to specific subcellular zones (Lowery et al., 2005; Strebhardt, 2010). Upon ablation of the kinase domain, the PBD domain alone becomes a dominant-negative form of PLKs (Seeburg et al., 2008). Despite their roles in cell cycle regulation, recent reports have suggested PLKs may possess additional cellular functions (Strebhardt, 2010). For example, Plk3 has been shown to suppress tumor angiogenesis, and *Plk3*$^{-/-}$ mice developed tumors in various organs at advanced age, with enhanced angiogenesis (Xu et al., 2012, 2010a, 2010b; Yang et al., 2008). Additionally, PLK2 has been observed to control dendritic spine sprouting and the density of synapses in neurons by governing RAP1 activity *via* the regulation of PDZ-GEF (Lee et al., 2011a, 2011b). Interestingly, previous studies have also revealed that human *PLK2* transcripts can be observed in human fetal lung, kidney, spleen and heart (Simmons et al., 1992), and additional expression analysis showed that *PLK2* may also be found more specifically expressed in the vascular system in early developmental stages (Duncan et al., 2001; Zhong et al., 2010), suggesting that PLK2 may also regulate vascular development. Thus, given its role in controlling RAP1 activity, we speculate that during vascular development, PLK2 may also serve to mediate lamellipodia formation and attachment to the ECM in ECs through regulating EC RAP1 function.

Here, we report that PLK2 is expressed in the vascular system and can control angiogenesis during vascular development by specifically regulating the EC lamellipodia but not filopodia formation. Using a combination of high-resolution *in vivo* imaging of zebrafish vascular development and a human umbilical vein endothelial cell (HUVEC) *in vitro* cell culture system, we observed that loss of *PLK2* function resulted in a reduction in EC sprouting and migration, whereas overexpression of *PLK2* promoted angiogenesis. Moreover, PLK2 appears to impart its function through the regulation of RAP1 to mediate focal adhesion and lamellipodia formation in migrating ECs. Overall, our data reveal a conserved PLK2-RAP1 pathway that is crucial to regulate endothelial tip cell behavior in order to ensure proper vascular development and patterning in vertebrates.

Material and methods

Zebrafish strains

Embryos and adult fish were maintained under standard laboratory conditions as described previously (Zhang et al., 2013). The following lines were used: *Tg(kdrl:mcherry-ras)*^{s896} (Chi et al., 2008), *Tg(kdrl:GFP)*^{s843} (Jin et al., 2005), *Tg(fli1a:EGFP)*^{y1} (Lawson and Weinstein, 2002), and *Tg(hsp70:dn-MAML-GFP)*^{fb10} (Zhao et al., 2014).

PLK2 sequence alignment

PLK2 sequence alignment was performed by ClustalW multisequence alignment as described (Hegarty et al., 2013).

Morpholino (MO) knockdown and rescue experiments

To knockdown plk2b function, we used an ATG-MO (MO1) against the 5′UTR adjacent to the translation start site of *plk2b* and a splicing MO (MO2) against the 3′ splice site of exon 2. The MO sequences are: MO1 (ATG-*plk2b*-MO): 5′-GCTGTGTGTTACTGTGCTTTCTGTC-3′ and MO2 (splicing-*plk2b*-MO): 5′-TATGCAGTGTTTATCCTACCTTCTC-3′. Five base pairs (bp) of the ATG MO was altered to create a control 5 bp mismatched MO, which did not cause any discernible phenotypes: (ATG-*plk2b*-control-MO): 5′-GCTcTcTGTTAgTGTcCTTTCTcTC-3′. One-cell stage *Tg(kdrl:mcherry-ras)*, *Tg(fli1a:eGFP)* embryos were injected with 10 ng of MO1, MO2 or control MO. To confirm that MO1 blocked the translation of *plk2b*, the following primers were used to PCR amplify a construct that fuses the *plk2b* 5′UTR region to GFP: *plk2b*-GFP-F: 5′-actgtgacagaaagcacagtaacacacagccATGGTGAGCAAGGGCGAGGA-3′ and GFP-R: 5′-TTACTTGTACAGCTCGTCCA-3′. This *5′UTR plk2b-GFP* construct was subcloned into the pCS2 vector, confirmed by sequencing and then transcribed into capped mRNA using a mMessage mMachine SP6 Transcription kit (Cat. no. AM1340, Life Technologies). 50 pg of the *5′UTR plk2b-GFP* RNA with or without 10 ng of *plk2b* MO1 was injected into zebrafish embryos at the one-cell stage. To evaluate the MO2 function, the following primers were used to detect *plk2b* exon 1-4 mRNA from 50 24 hpf (hour post-fertilization) control or MO2 injected embryos: *plk2b*-sMO-rtF: 5′-GGAAATGTTACTGCCGGGGA-3′, *plk2b*-sMO-rtR: 5′-CGTTTTGCGTCTGTTGCTGA-3′. For the dominant negative *plk2b* (*dn-plk2b*) experiments, the *plk2b* PBD domain fragment was cloned into the pCS2 vector and then *in vitro* transcribed using the mMessage mMachine SP6 Transcription kit (Cat. no. AM1340, Life Technologies). The following primers were used for PCR of the PBD domain: *plk2b*-PBDF 5′-ACTCAGGGCTTCATGCCAGAAACGC-3′, *plk2b*-PBDR: 5′-GTTGCATCGCTGCAGCAGCATGTTGA-3′. One-cell stage *Tg(kdrl:mcherry-ras)* or *Tg(fli1a:eGFP)* embryos were injected with 180 pg of *dn-plk2b* mRNA. For mRNA rescue experiments, the *plk2b* coding sequence (CDS), which does not include the *plk2b* ATG MO1 binding site, and the human *PLK2* CDS were cloned into the pCS2 vector and then *in vitro* transcribed using the mMessage mMachine SP6 Transcription kit (Cat. no. AM1340, Life Technologies). The following primers were used for PCR: *plk2b*-cdsF 5′-ATGGAGACACTAAGGAATAC-3′, *plk2b*-cdsR: 5′-TCAGTTGCATCGCTGCAGCAGCATG-3′, *hPLK2*-cdsF 5′-ATGGAGCTTTTGCGGACTAT-3′, *hPLK2*-cdsR: 5′-TCAGTTACATCTTTGTAAGA-3′. One cell stage *Tg(kdrl:mcherry-ras)* embryos were co-injected with 10 ng of *plk2b* MO1 or MO2 and 80 pg of zebrafish *plk2b* RNA, 80 pg of human *PLK2* RNA, or 100 pg, 160 pg of

the *constitutively active human RAP1* (*ca-RAP1*) RNA (G12V). For mRNA overexpression experiments, one cell stage *Tg(kdrl:mcherry-ras)* or *Tg (fli1a:eGFP)* embryos were injected with 160 pg of *plk2b* RNA or 80 pg of the *ca-RAP1* RNA. For all MO and RNA experiments, the average length of each ISV and the average number of branches per ISV were measured as described in *Zebrafish microscopy and imaging* section.

Cell culture and immunofluorescence

HUVECs were purchased from Lonza (Cat. no. CC-2157). Cells were cultured in Endothelial Basal Medium (Cat. no. CC-3121, Lonza) supplemented with 10% Fetal Calf Serum, bovine brain supplement, human recombinant epidermal growth factor, penicillin (50 U/ml) and streptomycin (50 μg/ml) (Cat. no. CC-4133, Lonza). Cells grown for 24 h on coverslips were fixed with 4% PFA for 10 min at 37 °C and processed for immunohistochemistry, which was performed using the following antibodies: anti-PLK2 (Cat. no. K2392, Sigma, 1:500), anti-pFAK (Cat. no. 611722, BD Biosciences, 1:500), anti-Integrin αVβ3 clone LM609 (Cat. no. MAB1976, Millipore, 1:500). Primary antibody incubations were followed by incubation with anti-rabbit (Cat. no. A11034, Life Technologies) or anti-mouse IgG Alexa 488 (Cat. no. A11029, Life Technologies). Alexa 568-conjugated phalloidin was used to detect F-actin (Cat. no. A12380, Life Technologies, 1:500) and DAPI (Cat. no. D9564, Sigma) was used to label nuclei. To quantitate the number of filopodia, lamellipodia, pFAK plaques, and integrin αVβ3 plaques in cell cultures, HUVECs were fixed with 4% PFA and stained with phalloidin, anti-pFAK and anti-integrin αVβ3, respectively. The number of filopodia (actin-rich finger-like protrusions crossing the cell edge), lamellipodia (regions of actin-rich fringe adjacent to the leading edge), pFAK plaques, and integrin plaques were counted for each cell ($n=10$). Quantitation of the leading edge recruitment of PLK2 protein was performed using ImageJ software (Bivona et al., 2006). Regions of identical size were drawn around an area at the leading edge and at the cytosol faraway from the leading edge. The fluorescence intensity was determined for these areas of interest at each time point. Nine regions were used to calculate each condition from nine cells.

Zebrafish microscopy and imaging

Confocal, fluorescence and bright-field microscopy, as well as live imaging of zebrafish were performed using a Nikon C2 confocal microscope, a Leica DM IL LED and a Leica M205 FA stereomicroscope as previously described (Hegarty et al., 2013). Zebrafish embryos were dechorionated, anesthetized with tricaine, and mounted laterally in 1% agarose/egg water on a glass-bottom Petri dish (MatTek). Because of its strong GFP brightness, *Tg(fli1a:EGFP)* transgenic line was used to perform time-lapse imaging as well as to track lamellipodia and filopodia extensions ($n=10$ control MO, 10 *plk2b* MO1, 10 *dn-plk2b* mRNA, and 10 *plk2b* mRNA). As previously described (Lamalice et al., 2007; Phng et al., 2013), filopodia are defined as finger-like protrusions that cross the cell membrane's edge and have widths <1 μm, and lamellipodia are defined as protrusions adjacent to the leading edge that have stronger and broader GFP signal and widths between 1 μm and 5 μm. To evaluate the relative ISV length as well as the number of filopodia, lamellipodia, and branching ECs in the zebrafish vasculature, three ISVs were measured from nine different embryos (total measured ISVs=27) for each condition.

Flow cytometry

Tg(kdrl:mcherry-ras) embryos were treated with SU5416 or DMSO from 20 to 32 hpf and collected at 32 hpf. *Tg(kdrl:mcherry-ras)* and *Tg(kdrl:mcherry-ras; Tg(hsp70:dn-MAML-GFP)* embryos were heat-shocked from 20 to 32 hpf and collected at 32 hpf. 100 embryos for each condition were collected to generate one biologic replicate for cell sorting. Disaggregation into single-cell suspension was achieved as previously described (Bertrand et al., 2010). Endothelial cell sorting was performed on a FACS Aria 2 (Becton Dickinson, San Jose, CA) and quantitiative PCR was performed using cDNA from 10,000 sorted endothelial cells per biological replicate to test *plk2b* expression.

Expression analysis, quantitative PCR and RT-PCR

Whole-mount *in situ* hybridization was performed on 16, 24, 36 and 48 hpf zebrafish embryos as described previously (Hegarty et al., 2013) using a *plk2a* and a *plk2b* RNA probe. The *plk2a* and *plk2b* RNA probes were generated by PCR, using the following primers: *plk2aF* 5′-TTCTTCGCCATGACTTTTTCTGCCA-3′, *plk2aR* 5′-cttgatttaggtgacactatagaaAAGCATCCTCGATTTCCCA-3′, *plk2b*F 5′-ACTCAGGGCTTCATGCCAGAAACGC-3′, *plk2b*R 5′-cttgatttaggtgacactatagaaGTTGCATCGCTGCAGCAGCATGTTGA-3′, *plk2b*senseF 5′-cttgatttaggtgacactatagaaACTCAGGGCTTCATGCCAGAAACGC-3′, *plk2b*senseR 5′-GTTGCATCGCTGCAGCAGCATGTTGA-3′. Using Power SYBR Green PCR Master Mix (Cat. no. 4367659, Life Technologies), *plk2b* quantitative PCR experiments were performed from cDNA obtained from three biologic replicate pooled samples containing flow cytometry sorted fish endothelial cells for each represented condition. Primer sequences used are as follows: *plk2a*RT-F 5′-GCAGACACCGTGGCCAGAGTACTA-3′ and *plk2a*RT-R 5′-GCAGGCTCATGTGAGTGCCATTGT-3′ *plk2b*RT-F 5′-ACAACACGGTGGGCGTCCTTT-3′ and *plk2b*RT-R 5′-TCAGCTGGAAGGTAGCGGACG-3′. *hPLK2* reverse transcriptase (RT)-PCR experiments were performed from cDNA obtained from HUVECs. Primer sequences used for human RT-PCR are as follows: *hPLK2*F 5′-GAATGCCTTGAAGACAGTACCA-3′ and *hPLK2*R 5′-TCAGTTACATCTTTGTAAGA-3′. DNA gel band intensity was quantified using ImageJ software.

Small molecule treatment with zebrafish embryos

The VEGF pathway inhibitor SU5416 (Cat. no. S8442, Sigma) and the Polo-like kinase inhibitor, BI 2536 (Cat. no. 45706, Sigma) (Steegmaier et al., 2007), were dissolved in DMSO (Cat. no. 472301, Sigma) and diluted to 400 μmol/L and 2 μmol/L with egg water, respectively, to make the stock solution. For *plk2b* zebrafish expression assay, 20 hpf WT embryos were placed in a solution with 1 ml of 50% DMSO or SU5416 stock solution and 19 ml of egg water (final concentration: 2 μmol/L SU5416 with 2.5% DMSO). Embryos were fixed 10 h post treatment and whole-mount *in situ* hybridization was performed as described previously (Hegarty et al., 2013). For Polo-like kinase inhibition assay, 20 hpf *Tg(kdrl:GFP)* embryos were placed in a solution with 1 ml of DMSO or BI 2536 stock solution and 19 ml of egg water (final concentration: 100 nmol/L) and imaging was performed 28 h post treatment.

Heat shock experiments with zebrafish embryos

Tg(hsp70:dn-MAML-GFP) embryos were initially heat-shocked at 20 hpf in a 42° water bath for 5 min, which was subsequently repeated for every 4 h until 32 hpf. GFP positive and negative labeled embryos were then fixed seperately at 32 hpf, and whole-mount *in situ* hybridization was performed as described previously (Hegarty et al., 2013).

siRNA transfections

The following human *PLK2* siRNA (5′-GGACATGGCTGTGAATCAG-3′), which was previously confirmed to target human *PLK2* (Lim

et al., 2015; Mbefo et al., 2010; Warnke et al., 2004), as well as a non-targeting control siRNA (scrambled sequence) were purchased from Dharmacon. HUVECs were transfected using Lipofectamine RNAiMAX (Cat. no. 13778030, Life Technologies) according to the manufacturer's instructions.

Lentivirus production and endothelial cell transductions

Lenti-X 293T cells (Cat. no. 632180, Clontech Laboratories) were plated in 100 mmol/L dishes and incubated overnight. The cells were then transfected with second generation viral packaging vectors (Cat. no. TLP5912, Thermo scientific) as well as pWPI empty vectors (control) (Addgene plasmid 12254) or pWPI vector containing a *ca-RAP1* expression cassette or *dn-PLK2* (which only contains *PLK2* PBD domain) expression cassette before the *IRES-eGFP* cassette. Virus-containing supernatant was collected after 48 h, then filtered through a 0.45 μmol/L pore-size filter and supplemented with 5 mg/ml polybrene. The filtered virus-containing supernatants were then added to HUVECs that were seeded in 6-well plates one day before transduction, and then incubated overnight. Two days after transduction, the transduction efficiency was checked by GFP signal. This procedure typically resulted in infection of more than 90% of cells. Successfully transduced GFP positive HUVECs were then used for subsequent assays.

Two-dimensional tube formation assay

Basement membrane matrix (Cat. no. 356234, BD Biosciences) was thawed at 4 °C overnight and diluted with an equal volume of serum-free Endothelial Basal Medium (Cat. no. CC-3121, Lonza). Each well of a 96-well plate was coated with 100 μl of mixed matrix, and then incubated for 30 min at 37 °C. HUVECs transfected with control siRNA, *PLK2* siRNA or *ca-RAP1* virus were plated on this matrix-coated well, and then allowed to adhere and migrate for 4 h at 37 °C. Tube formation was quantified by counting the length of formed tubes using 100 × magnification pictures that were captured and processed as described above. Each sample was assayed in two to three random fields and independently repeated three times.

Wound healing assay

HUVECs transfected with control siRNA, *PLK2* siRNA or *ca-RAP1* virus were seeded on 8-well chamber slides. To create an injury to the HUVEC monolayer, this cell monolayer was scraped with sterile pipette tips 48 h after transfection, and then washed twice with PBS to remove floating cells. Photographs were taken 2 h and 14 h after wound formation, and the cell-free area percentage of each image was measured between these two time-points to calculate the wound closure ratio. Each sample was assayed in two to three random fields and independently repeated three times.

Transwell migration assay

HUVECs transfected with control siRNA, *PLK2* siRNA or *ca-RAP1* virus were counted and seeded on membrane inserts (8 μm pore size) (Cat. no. 3421, Costar) in the presence of 200 μl of Endothelial Basal Medium supplemented with 0.1% BSA. The lower chamber contained 800 μl of Endothelial Basal Medium supplemented with 4% Fetal Calf Serum. Following a four hour incubation, cells that had migrated into the lower compartment were fixed in methanol for 10 min and stained with Crystal Violet for 10 min. Transmigrated cells were counted under a Leica M205 FA stereomicroscope. Each sample was assayed in two to three random fields and independently repeated three times.

HUVEC adhesion assay

Glass coverslips were coated with type I collagen (Cat. no. 354236, BD Biosciences, 10 μg/ml) or fibronectin (Cat. no. 354008, BD Biosciences, 5 μg/ml), and incubated one hour at 37 °C. HUVECs were trypsinized, and 3000 cells were seeded per coverslip. After 50 min incubation at 37 °C, the adherent HUVECs were fixed with 4% paraformaldehyde, and cell numbers were counted with DAPI staining.

HUVEC proliferation assay

To detect proliferating cells, HUVECs transfected with control or *PLK2* siRNA were counted and seeded on 4-well chamber slides and incubated with 10 μM 5-bromo-2′-deoxyuridine (BrdU, Cat. no. B5002, Sigma) for 6 h. HUVECs were then fixed with 4% PFA and imaged by immunofluorescence microscopy using an antibody against BrdU (Cat. no. OBT0030, abdserotec) which was then detected with a secondary antibody conjugated to Alexa Fluor 568. The percentage of cells undergoing proliferation was determined by dividing the number of BrdU positive cells by the total number of cells labeled with DAPI nuclear stain.

HUVEC cell death assay

HUVECs transfected with control or *PLK2* siRNA were counted and seeded on 4-well chamber slides and grown for 48 h. Transfected HUVECs were then fixed with 4% PFA and apoptotic cells were detected using an *in situ* cell death detection kit from Roche (# 2156792). The percentage of cells undergoing apoptosis was determined by dividing the number of TUNEL positive cells by the total number of cells labeled with DAPI nuclear stain.

HUVEC RAP1 activity assay

RAP1 activity was measured using the RAP1 activation assay kit (Cat. no. 17-321, Millipore), which is based on the specific binding of a GST fusion protein containing the Rap-binding domain of RalGDS (RBD-GST) to the active GTP-bound form of RAP1. Briefly, the GTP-bound RAP1 was pulled down using RBD-GST, which was immobilized to glutathione agarose beads. Precipitated GTP-bound RAP1 and total RAP1 as input control were identified by SDS-PAGE (12%) gels and western blot using a polyclonal anti-RAP1 antibody. RAP1-GTP and total RAP1 band intensities were quantified using ImageJ software.

Western blot analysis

Western blots were performed according to the manufacturer's instructions using the following primary antibodies: anti-PLK2 (Cat. no. K2392, Sigma, 1:1000), anti-GAPDH (Cat. no. GT239, GeneTex, 1:500) and anti-PDZ-GEF1 (Cat. no. WH0009693M1, Sigma, 1:1000). Gel band intensity was quantified using ImageJ software.

PLK2 and PDZ-GEF1 co-immunoprecipitation assay

HUVECs were rapidly lysed at 4 °C, and the whole-cell lysates were precleared with protein A-agarose beads (Cat. no. 11719408001, Roche) for three hours at 4 °C. The supernatants were incubated overnight at 4 °C with 1 μg of rabbit anti-PLK2 antibody (Cat. no. K2392, Sigma) or rabbit immunoglobulin G (IgG) as a negative control. On the next day, 50 μL of protein A-agarose beads was added to the immunoprecipitation tube and incubated at 4 °C for three hours. After washing, the bead/protein complexes were boiled in sample loading buffer and then identified by SDS-

PAGE and western blot using anti-PDZ-GEF1 (Cat. no. WH0009693M1, Sigma).

Statistical analyses

Quantitative statistical data are shown as the mean ± standard error of the mean (SEM) for 3 to 4 separate experiments. *P*-values of group comparisons were obtained by using unpaired two tailed Student's *t*-test analysis. Multi-group statistical significance was evaluated by one-way analysis of variance (ANOVA) with Turkey's multiple comparison test. Statistical significance was concluded when *P*-values were < 0.05.

Results

Endothelial cell expression of PLK2 is conserved in vertebrates

Because PLK2 has been recently reported to regulate RAP1 activity in neurons (Lee et al., 2011a, 2011b) and RAP1 is required for angiogenesis (Carmona et al., 2009; Lakshmikanthan et al., 2011), we postulated that PLK2 may also mediate endothelial cell sprouting. Thus, we initially examined the expression of *PLK2* in both HUVECs and the developing zebrafish vasculature (Fig. 1; Figs. S1 and S2). Reverse transcription (RT)-PCR and western blot analysis revealed that *PLK2* transcript and protein, respectively, were expressed in HUVECs (Fig. S1A–C). Furthermore, immunohistochemistry showed that PLK2 can also aggregate in regions of the lamellipodia of migrating HUVECs as detected by the colocalization of PLK2 with the thick cortical network of actin filaments in the extending EC membrane (Fig. 1A–C, arrowheads). Protein sequence comparison using the ClustalW program revealed that *PLK2* is highly conserved across vertebrate species (Fig. S3A) and genetic analysis showed that the *plk2* zebrafish ortholog may be gene duplicated, resulting in a *plk2a* and a *plk2b* gene on chromosome 10 and 8, respectively (Fig. S3B and C). Additionally, zebrafish Plk2a and Plk2b proteins share 74% and 70% homology with human PLK2, and *plk2b* appeared to be more closely syntenic than *plk2a* to mammalian *PLK2* (Fig. S3B). Whole mount *in situ* analysis showed that *plk2b* was expressed predominantly in the developing vasculature further supporting the conserved EC role of PLK2 (Fig. 1D–F, Fig. S2), whereas *plk2a* appeared to be mainly expressed in the nervous system consistent with PLK2's function in neurons (Fig. S4A–D, yellow arrowheads). As a result, we focused on the role of zebrafish Plk2b to further understand the role of PLK2 in vascular development.

Because VEGF and Notch signaling can promote and inhibit angiogenesis, respectively, we investigated whether these signaling pathways may alter *PLK2* expression. As a result, we observed that both *PLK2* transcript and protein levels were increased in VEGF-treated HUVECs (Fig. S1A–C), whereas zebrafish embryos treated with the VEGF inhibitor SU5416 at 20 hpf exhibited significantly reduced *plk2b* EC expression by 32 hpf (Fig. S1E and H). In contrast, Notch inhibition in Tg(*hsp70:dn-MAML-GFP*) zebrafish

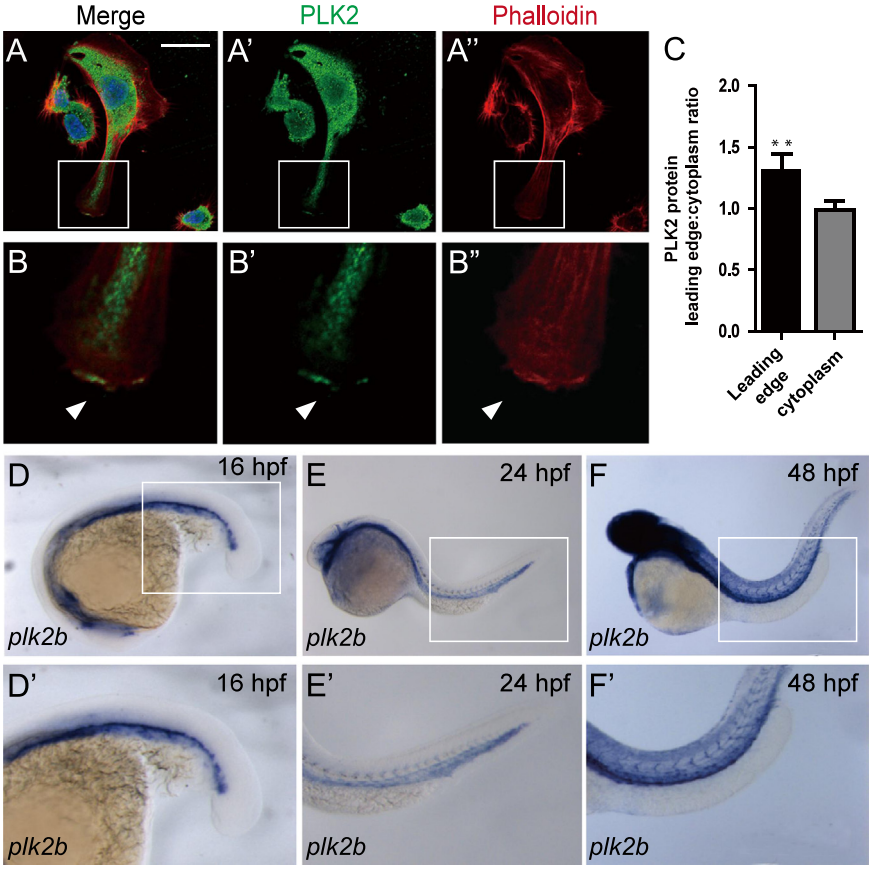

Fig. 1. PLK2 is expressed in endothelial cells. (A–B″) Immunostaining of HUVECs reveals that PLK2 is expressed in ECs. (B–B″) Enlarged image of the boxed area in A–A″ shows that PLK2 can aggregate at the leading edge of extending ECs (arrowhead). (A and B)-merge; (A′ and B′)-anti-PLK2 immunostaining (green); (A″ and B″)-phalloidin actin staining (red). DAPI nuclear staining (blue). Scale bar, 40 μm. (C) Quantitative measurements of PLK2 localized at the leading edge and in the cytoplasm of HUVECs (Mean ± s.e.m. *$p=0.0056$ by Student's *t*-test). (D–F) *in situ* hybridization shows that *plk2b* is expressed in the zebrafish vasculature at 16 hpf ($n=31/31$), 24 hpf ($n=46/47$), and 48 hpf ($n=28/30$). (D′–F′) Enlarged image of the boxed area of D–F shows that *plk2b* is expressed in the cardinal vein, aorta, and intersomitic vessels of the zebrafish body and tail.

embryos at 20 hpf resulted in increased *plk2b* expression by 32 hpf (Fig. S1G and I). Finally, we observed that expression of *plk2b*, but not *plk2a*, was overall significantly downregulated by *in situ* and quantitative PCR in *cloche* mutants which lack ECs (Stainier et al., 1995) (Fig. S5).

PLK2 is required for endothelial cell sprouting and migration

Because of its EC expression and localization at the leading edge of sprouting ECs, we next performed *PLK2* knockdown and overexpression experiments *in vivo* and *in vitro* in zebrafish and HUVECs, respectively, to investigate whether *PLK2* could regulate EC sprouting and migration. To this end, we generated a *plk2b* ATG MO (MO1) and a *plk2b* splice MO (MO2), which target the translation initiation site and its surrounding sequences and the splice junction boundary sequences between exon 2 and intron 2, respectively (Fig. S6A–H). 10 ng of either MO1 or MO2 injected into zebrafish *Tg(kdrl:mcherry-ras)* embryos, in which endothelial cells are labeled in red, resulted in a significant reduction in intersomitic vessel (ISV) length (Fig. 2B, C and I; Fig. S6I). In particular, some ISVs failed to migrate dorsally beyond the horizontal myoseptum to form the dorsal longitudinal anastomotic vessel (DLAV) (Fig. 2B, C and open arrowheads). Furthermore, injecting dominant negative *plk2b* RNA (*dn-plk2b*), which lacks the Plk kinase domain, into *Tg(kdrl:mcherry-ras)* zebrafish embryos or treating *Tg(kdrl:GFP)* zebrafish embryos with the polo-like kinase inhibitor, BI 2536, could also reduce ISV length (Fig. 2D and I; Fig. S6I and K). Finally, we observed that these loss of *plk2b* function embryos appeared to otherwise develop and swim normally compared to age-matched MO controls (Fig. S7), supporting that the phenotypic defects of the loss of *plk2b* function embryos were vascular-specific.

To validate the effect of the *plk2b* MOs, we attempted to rescue the *plk2b* morphant knockdowns by co-injecting zebrafish *plk2b* or human *PLK2* RNA. Co-injecting 80 pg of wild-type zebrafish *plk2b* mRNA or human *PLK2* mRNA with *plk2b* MOs significantly reduced the ability of *plk2b* MOs to cause the EC sprouting defect (Fig. 2E, F and I; Fig. S6I), in effect rescuing the *plk2b* MO knockdowns. Although injecting 80 pg of wild-type *plk2b* into zebrafish wild-type embryos had no effect on zebrafish development (Fig. 2G), injecting 160 pg of wild-type *plk2b* interestingly led to increased endothelial ISV branching and connections between neighboring ISVs at the horizontal myoseptum (Fig. 2H, J and arrowheads; Fig. S6I).

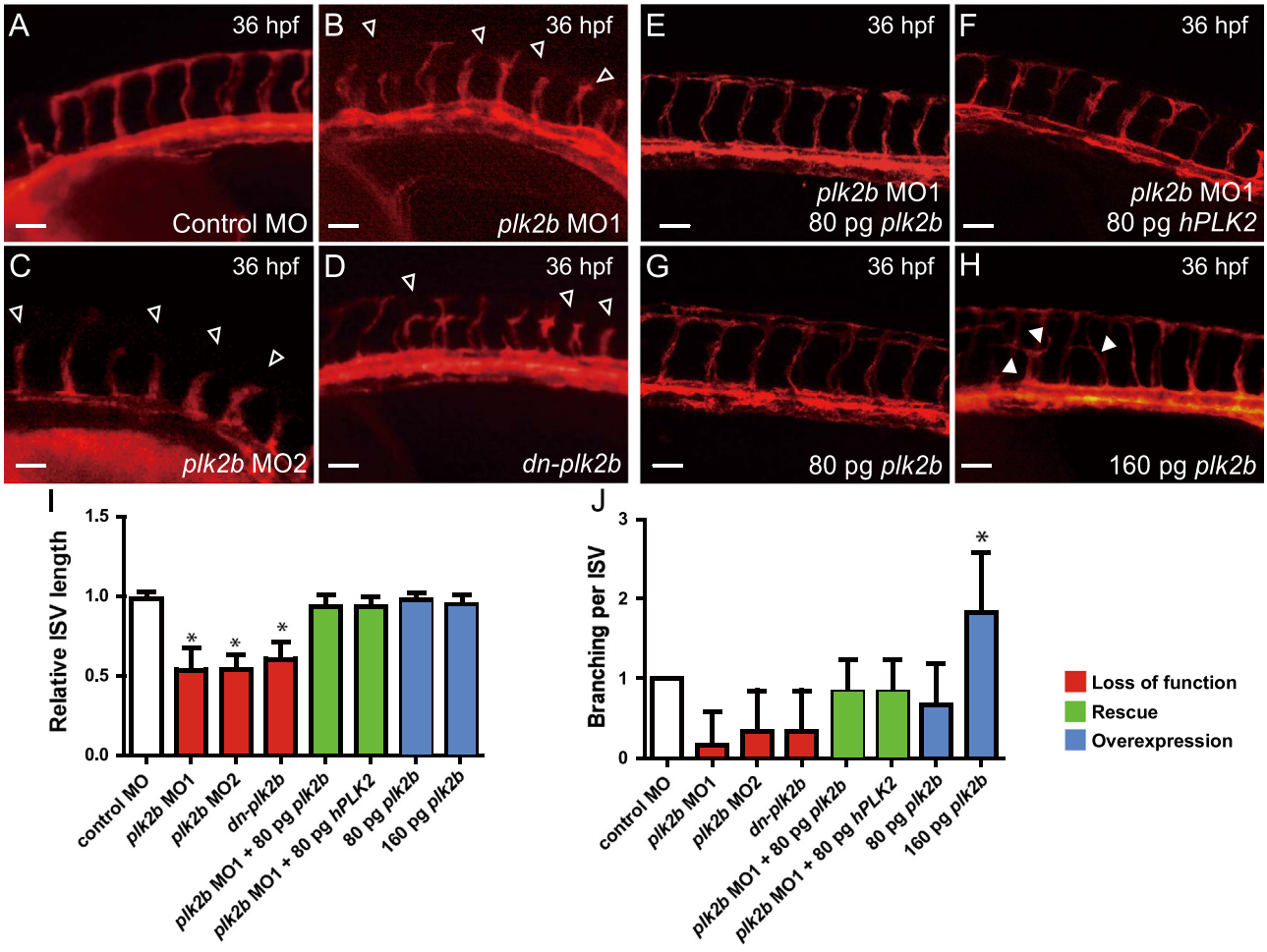

Fig. 2. *plk2b* regulates endothelial cell sprouting. (A–D) Fluorescence micrographs show that loss of *plk2b* function in *Tg(kdrl:mcherry-ras)* zebrafish embryos results in underdeveloped intersomitic vessel sprouting (open arrowheads) at 36 hpf. (A) control MO ($n=0/149$); (B) *plk2b* ATG MO (MO1) ($n=125/171$); (C) *plk2b* splice MO (MO2) ($n=89/137$); (D) *dn-plk2b* RNA – dominant negative *plk2b* ($n=49/85$). Injecting (E) 80 pg of *plk2b* ($n=31/103$) or (F) 80 pg of *hPLK2* ($n=24/71$) can rescue the *plk2b* MO1 vascular sprouting defect. (G) Injecting 80 pg of *plk2b* RNA into wild-type *Tg(kdrl:mcherry-ras)* embryos did not cause any significant vascular phenotypes ($n=0/105$). However, (H) injecting 160 pg of *plk2b* resulted in increased ISV spouting and branches (arrowheads) ($n=91/145$). Top, dorsal longitudinal anastomotic vessel (yellow asterisk); bottom, dorsal aorta/cardinal vein. Scale bar, 80 μm. Quantitative measurements of (I) intersomitic vessel length and (J) the number of ISV branches for each corresponding condition. Mean ± s.e.m. $^{*}p < 0.05$ by ANOVA.

To further analyze the direct effects of PLK2 deficiency on EC migration, we disrupted *PLK2* function in HUVECs using a *PLK2* siRNA that has been shown to successfully inhibit PLK2 protein expression in human cells (Lim et al., 2015; Mbefo et al., 2010; Warnke et al., 2004). When compared to control siRNA, *PLK2* siRNA knockdown inhibited the ability of VEGF and bFGF stimulated HUVECs to form a network of interconnecting branches as well as to migrate as detected in *in vitro* tube formation assays and transwell migration assays, respectively (Fig. 3A–D, G and H). Additionally, using wound healing assays where confluent monolayer cultures of HUVECs were wounded with a pipette tip, we observed that *PLK2* siRNA HUVECs exhibited significantly delayed migration and wound healing closure when compared to controls (Fig. 3E–F′ and I). To confirm that the delay in wound healing was due to a cell migration defect rather than a cell proliferation or cell death defect, we performed BrdU labeling and TUNEL staining experiments and observed no significant difference in cell proliferation or cell apoptosis between *PLK2* and control siRNA knockdowns (Fig. 3J and K). Finally, we transfected HUVECs with human dominant negative *PLK2* RNA (*dn-PLK2*) to confirm the *PLK2* siRNA findings and discovered that *dn-PLK2* RNA can also block the endothelial cell migration in *in vitro* tube formation, transwell migration and wound healing assays (Fig. S8). Together, these studies show that PLK2 functions to regulate the migration of endothelial cells *in vivo* and *in vitro*.

PLK2 regulates lamellipodia but not filopodia formation through mediating EC cell adhesion

Angiogenesis is dependent on the initiation and stabilization of EC cell membrane extensions to form sprouting EC branches. In order to further investigate how *PLK2* may regulate angiogenesis, we examined both filopodia and lamellipodia formation *in vivo* using time-lapse imaging of the zebrafish vasculature as well as *in vitro* using HUVECs. We observed that loss of *plk2b* function in zebrafish *Tg(fli1a:eGFP)* embryos and loss of *PLK2* function in HUVECs resulted in significantly reduced lamellipodia numbers when compared to controls (Fig. 4A, B, G and H; Fig. S9A–C; Movie S1–S3). Conversely, in zebrafish overexpressing *plk2b*, we observed increased lamellipodia numbers and endothelial branches (Fig. 2H and J; Fig. 4G; Fig. S6I; Fig. S9D, Movie S4). However, we did not observe a significant difference in filopodia numbers after perturbing PLK2 function in HUVECs and zebrafish embryos (Fig. 4G, H).

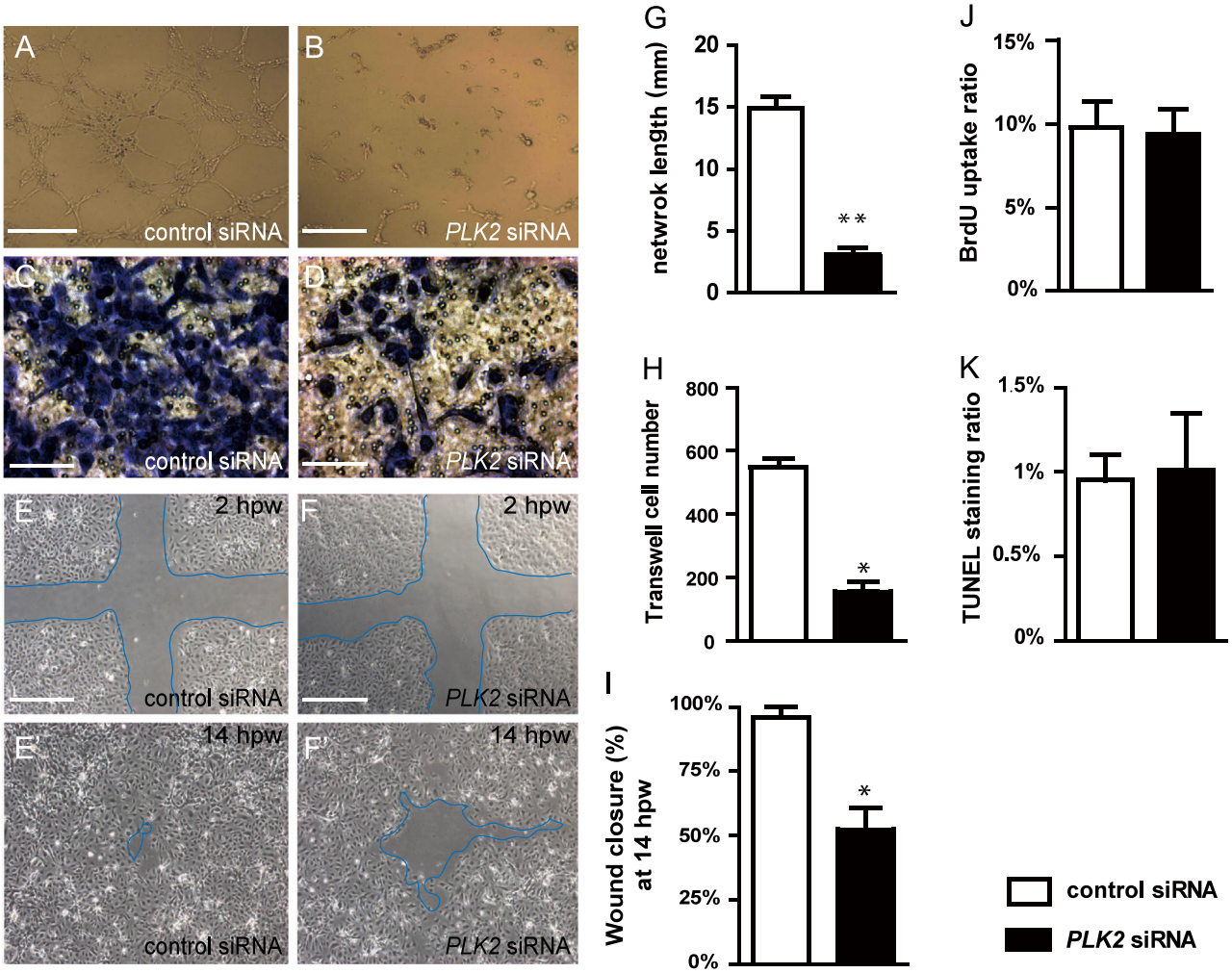

Fig. 3. *PLK2* regulates endothelial cell migration. (A and B) EC tube formation assays, (C and D) transwell EC migration assays, and (E–F′) wound healing EC assays show that when compared to control siRNA knockdown, *PLK2* siRNA knockdown in HUVECs results in (B and G) decreased EC network/tube formation ($p=0.0028$), (D and H) reduced EC migration formation ($p=0.0185$), and (F, F′ and I) slower EC wound healing/closure, respectively ($p=0.0114$). (J and K) Quantitative measurements of the percentage of (J) BrdU positive cells and (K) TUNEL staining positive cells in control and *PLK2* siRNA transfected HUVECs show that PLK2 knockdown does not affect HUVEC cell proliferation ($p=0.6007$) and apoptosis ($p=0.7970$). (A, B, E–F′) Scale bar, 1.6 mm. (C and D) Scale bar, 400 μm. hpw – hours post wounding. Mean ± s.e.m. $^{*}p<0.05$, $^{**}p<0.01$ by Student's *t*-test.

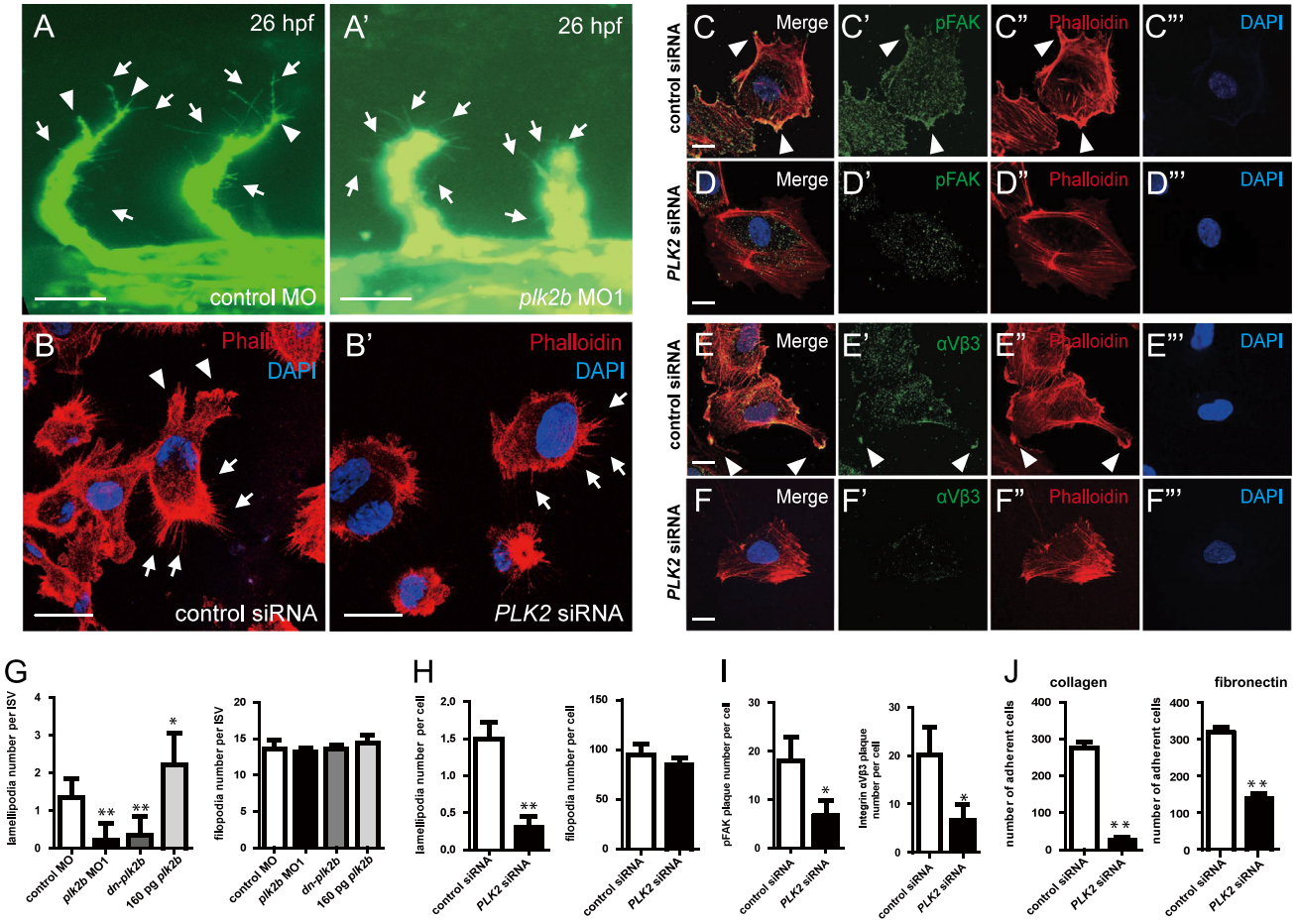

Fig. 4. *PLK2* regulates endothelial cell lamellipodia and cell adhesion formation. (A–A′) 26 hpf *plk2b* MO1 injected *Tg(fli1a:eGFP)* fish ($n=31/40$) exhibit fewer lamellipodia, and extending intersomitic vessels compared to age-matched control MO injected *Tg(fli1a:eGFP)* fish ($n=0/48$). Scale bar, 40 μm. Top, dorsal longitudinal anastomotic vessel; bottom, dorsal aorta/cardinal vein. (B–B′) Phalloidin staining reveals that *PLK2* siRNA transfected HUVECs display reduced lamellipodia when compared to control siRNA transfected HUVECs. Scale bar, 20 μm. Immunostaining of (C–C‴, D–D‴) pFAK and (E–E‴, F–F‴) integrin αVβ3 shows that focal adhesions and integrins, respectively, are localized to the lamellipodia of migrating/extending (C and E) control siRNA transfected HUVECs, but they fail to organize and aggregate in (D and F) *PLK2* siRNA transfected HUVECs. Scale bar, 10 μm. (G) Quantitative measurements of the number of lamellipodia and filopodia reveal that zebrafish *plk2b* knockdowns have reduced lamellipodia but relatively the same number of filopodia (finger-like protrusions crossing the cell edge) when compared to controls. Conversely, zebrafish RNA injection of 160 pg *plk2b* resulted in more lamellipodia only. (H) Quantitative measurements of the number of lamellipodia and filopodia reveal that human *PLK2* knockdowns have reduced lamellipodia ($p=0.0023$) but relatively the same number of filopodia ($p=0.2615$) when compared to controls. (I) Quantitative measurements of the number of pFAK ($p=0.0143$) and integrin αVβ3 plaques ($p=0.0224$) reveals that knockdown of *PLK2* reduced the number of cell adhesions in HUVECs. (J) EC adhesion assays show that *PLK2* siRNA HUVECs adhered less to type I collagen ($p=0.0017$) and fibronectin-coated coverslips ($p=0.0061$) compared to control siRNA HUVECs. Arrowheads and arrows point to lamellipodia and filopodia, respectively. Red – phalloidin/actin staining; Blue – DAPI staining; Green – (A) GFP, (C–D) pFAK, or (E and F) integrin αVβ3. Mean ± s.e.m. $^{*}p<0.05$, $^{**}p<0.01$ by ANOVA for G and Student's *t*-test for H–J.

Because integrin-dependent focal adhesions help to stabilize and maintain EC lamellipodia protrusions during angiogenesis, we next examined the localization of phosphorylated focal adhesion kinase (pFAK) and integrin αVβ3 in control and *PLK2* siRNA transfected HUVECs. *PLK2* siRNA transfected HUVECs failed to form stable cell adhesion plaques as detected by pFAK and integrin αVβ3 immunostaining and to organize actin filaments to develop a leading edge for lamellipodia protrusions (Fig. 4C–F and I). As a result, we observed reduced numbers of *PLK2* siRNA transfected HUVECs adhering to either collagen or fibronectin coated coverslips (Fig. 4J). Overall, these studies reveal that PLK2 may mediate angiogenesis through regulating EC adhesion and lamellipodia stabilization.

Supplementary material related to this article can be found online at http://dx.doi.org/10.1016/j.ydbio.2015.05.011.

RAP1 acts downstream of PLK2 to regulate endothelial cell sprouting and migration

Previous studies have shown that PLK2 can mediate sprouting in neuronal cells through regulating the ability of PDZ-GEF1 to exchange GDP for GTP on RAP1 and thereby activating RAP1 (Lee et al., 2011b). Because RAP1 has also been recently reported to mediate angiogenesis through the phosphorylation of FAK and the subsequent activation of integrins (Carmona et al., 2009), we investigated whether PLK2 may regulate RAP1 during EC focal adhesion formation and EC migration. Using a RAP1-GTP binding assay (de Rooij and Bos, 1997), which monitors RAP1 activity through the analysis of RAP1-GTP binding to a GST fusion protein containing the RAP-binding domain (RBD) of RalGDS (RBD-GST), we examined the levels of activated RAP1-GTP in *PLK2* and control siRNA transfected HUVECs. As a result, we observed reduced activated RAP1-GTP in *PLK2* siRNA transfected HUVECs when compared to controls, suggesting that PLK2 may be required to activate RAP1 (RAP1-GTP) in ECs to bind to its effector (Fig. 5A and B). Finally, to investigate whether PLK2 in ECs may regulate RAP1 activity through PDZ-GEF1 as observed in neurons, we performed PLK2 immunoprecipitations in HUVECs and observed that PDZ-GEF1 could interact in a protein complex with PLK2 (Fig. 5C).

Because these data suggest that PLK2 may interact with PDZ-GEF to activate Rap1 to mediate focal adhesion assembly, we

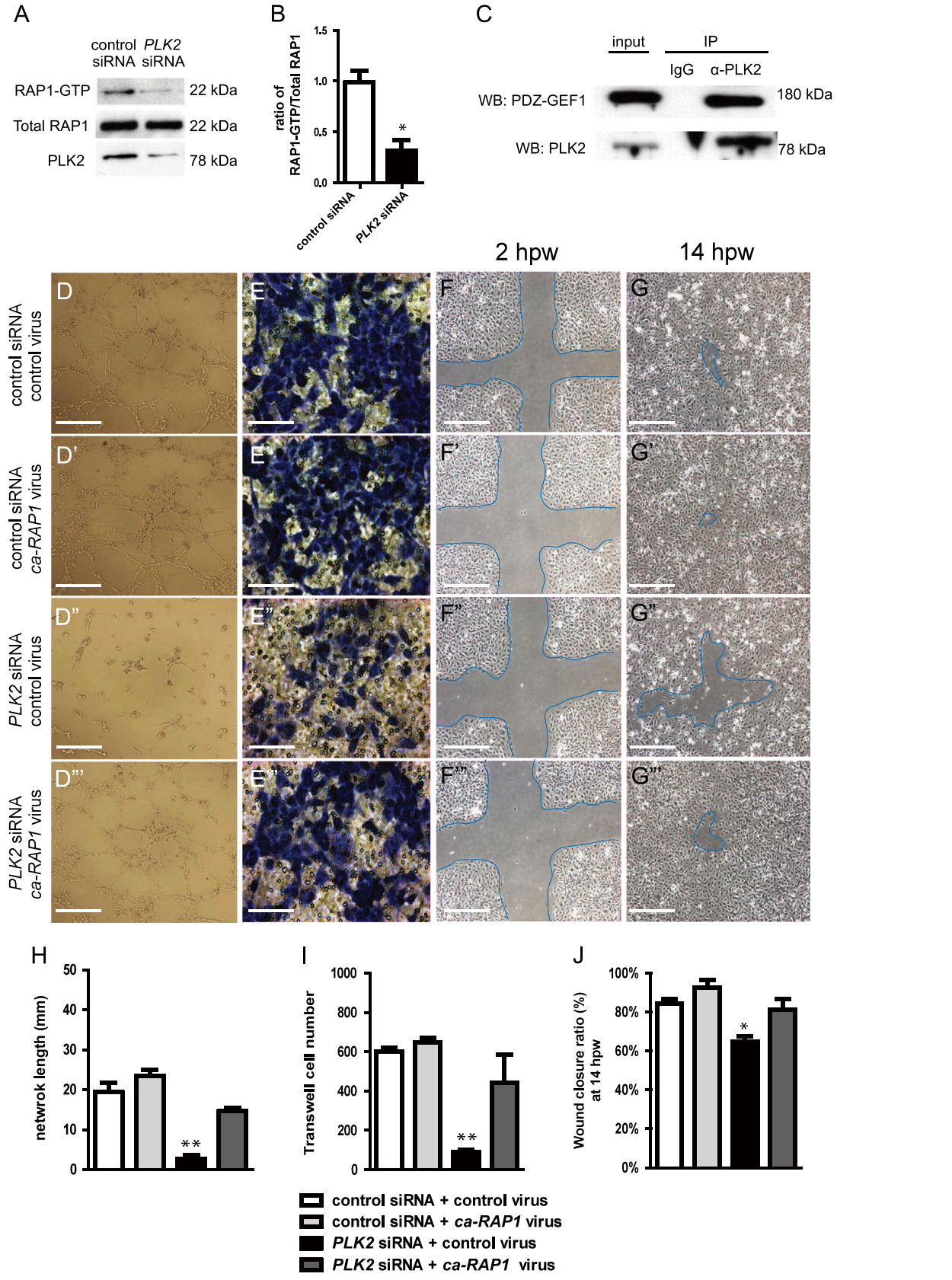

Fig. 5. *PLK2* regulates HUVEC migration *in vitro via* RAP1 activity. (A) RAP1 immunoblot of RAP1-GTP binding assays shows that there is less RAP1-GTP in *PLK2* siRNA HUVECs than in control siRNA HUVECs (22 kDa). PLK2 immunoblot shows the efficiency of *PLK2* siRNA knockdown in HUVECs. (B) Quantitative measurements show that the ratio of RAP1-GTP/Total RAP1 is less in *PLK2 siRNA* (Mean ± s.e.m. $^{*}p=0.015$ by Student's *t*-test). (C) Immunoprecipitation (IP) of HUVEC lysates with anti-PLK2 antibody reveals that PLK2 interacts in a complex with PDZ-GEF1 (180 kDa). Western analyses of immunoprecipitations were performed with anti-PDZ-GEF (WB: PDZ-GEF) and anti-PLK2 antibodies (WB: PLK2). IP IgG – control antibody; α-PLK2 – anti-PLK2 antibody. (D) EC tube formation assays, (E) Transwell EC migration assays, and (F and G) wound healing EC assays show that *ca-RAP1* virus can rescue the *PLK2* siRNA knockdown HUVEC (compare D″ to D‴) EC network/tube formation, (compare E″ to E‴) cell migration, and (compare F″, G″ to F‴, G‴) wound healing defects. (D–D‴, F–F‴, G–G‴) Scale bar, 1.6 mm. (E–E‴) Scale bar, 400 μm. (H–J) Quantitative measurements were performed on (H) EC tube formation assays, (I) transwell EC migration assays, and (J) wound healing EC assays. hpw-hours post wounding. Mean ± s.e.m. $^{*}p<0.05$, $^{**}p<0.01$ by ANOVA for H–J.

investigated whether a constitutively active RAP1 (ca-RAP1) (Brinkmann et al., 2002) protein might be able to rescue the *PLK2* knockdown angiogenesis phenotype. To this end, we infected the *ca-RAP1* virus into *PLK2* siRNA HUVECs and discovered that the *ca-RAP1* virus could partially rescue the EC migration and sprouting defects observed in *PLK2* knockdown HUVECs (compare Fig. 5D″–G″ to D‴–G‴, H–J). Additionally, we attempted to rescue the zebrafish *plk2b* MO knockdowns with *ca-RAP1* RNA. Co-injecting 100 pg of *ca-RAP1* RNA with *plk2b* MO1 significantly reduced the ability of *plk2b* MO1 to cause the EC sprouting defect (Fig. S10A; Fig. S6I), in effect rescuing the *plk2b* MO1 knockdowns. Moreover, co-injecting higher amounts of *ca-RAP1* RNA (160 pg) led to not only rescue of the *plk2b* MO1 EC defect, but also some ectopic EC sprouting into the somites (Fig. S10B, yellow arrowheads and D; Fig. S6I). Consistent with these findings, injecting 80 pg of *ca-RAP1* RNA into wild-type embryos also resulted in ectopic EC sprouting as well (Fig. S10C, yellow arrowheads and D; Fig. S6I). To investigate how ca-RAP1 might rescue the *PLK2* knockdown HUVEC migration defects, we examined the ability of *ca-RAP1* infected *PLK2* siRNA HUVECs to develop focal adhesions. We discovered that the *ca-RAP1* virus could rescue the reduced numbers of focal adhesions as well as the type I collagen and fibronectin cell adhesion defects in *PLK2* siRNA HUVECs when compared to control virus infected *PLK2* siRNA HUVECs (compare Fig. 6C, G to D, H; Fig. S11A–D). Although *ca-RAP1* could rescue the *PLK2* knockdown angiogenesis phenotype through restoring lost focal adhesions in HUVECs, interestingly, we did not observe a significant increase in EC sprouting, migration and focal adhesion formation between control and *ca-RAP1* infected HUVECs (compare Fig. 5D–G to D′–G′ and H–J; Fig. 6A, E to B, F; Fig. S11A and B), suggesting that RAP1 may be required but not sufficient for EC sprouting *in vitro*. Overall, these studies reveal that PLK2 may mediate angiogenesis through regulating RAP1 activity and localization.

Discussion

Angiogenesis is dependent on endothelial tip cells to lead new blood vessels during vascular development. In response to guidance cues, these endothelial tip cells directionally extend their membranes through a series of organized cellular processes including the development of filopodia and lamellipodia. Here, we show that PLK2 specifically regulates EC lamellipodia but not filopodia formation to direct EC sprouting and angiogenesis. Consistent with its recently reported role in neurons (Lee et al., 2011a, 2011b), we observed that PLK2 can control RAP1 activity in ECs. Although it remains unclear as to precisely how PLK2 may regulate neuronal sprouting, we discovered that in ECs, PLK2 interacts with PDZ-GEF to activate RAP1 in order to regulate the formation of EC focal adhesions and the subsequent growth of lamellipodia. Similar to the loss of RAP1 function EC defects (Carmona et al., 2009; Lakshmikanthan et al., 2011), loss of PLK2 function results in reduced EC attachment, lamellipodia structures, and overall angiogenesis.

Previous studies have reported that *PLK2* is expressed in Xenopus and mouse embryonic brains and blood vessels (Duncan et al., 2001; Visel et al., 2004). Furthermore, it has been shown to be more than 2.5-fold greater in mouse tip ECs than in stalk ECs (del Toro et al., 2010). In line with these findings, we discovered that *PLK2* is also expressed in both HUVECs and the zebrafish vasculature and is further regulated by the VEGF and Notch signaling pathways, which are known to control angiogenesis. Thus, these findings suggest that *PLK2*'s function may be conserved across vertebrates to regulate blood vessel formation.

In support of its role in angiogenesis, *PLK2* knockdowns resulted in EC sprouting and migration defects in both HUVECs and zebrafish. Because PLK2 was previously shown to regulate RAP1 through interactions with PDZ-GEF in neurons (Lee et al., 2011b) and RAP1 is crucial for EC sprouting (Carmona et al., 2009; Chrzanowska-Wodnicka et al., 2008; Lakshmikanthan et al., 2011; Wei et al., 2007), we attempted to rescue the *PLK2* knockdown EC defect using a constitutively activated RAP1 (ca-RAP1) protein. We discovered that ca-RAP1 could partially rescue this phenotype suggesting that PLK2 may regulate more than RAP1 activity during EC sprouting and migration. Given that other small GTPases, including RhoA, Rac1, and Cdc42, have been reported to regulate endothelial tip cell filopodia, lamellipodia, cell adhesion, and stress fiber formation (Kiosses et al., 2001; Spindler et al., 2010; Wojciak-Stothard et al., 1998), it is possible that PLK2 may regulate these other small GTPases through interactions with their respective GEFs. In particular, we postulate that a likely additional candidate that PLK2 may regulate would be Rac1 because of its role in lamellipodia formation. Finally, it is noteworthy that ca-RAP1 in control ECs did not result in a significant increase in EC sprouting, suggesting that RAP1 is required but not sufficient for EC sprouting. Thus, it will be particularly interesting in the future to examine whether PLK2 may regulate other small GTPases during angiogenesis.

Actin-rich filopodia and lamellipodia protrusions have been proposed to drive EC sprouting and vascular patterning. Filopodia

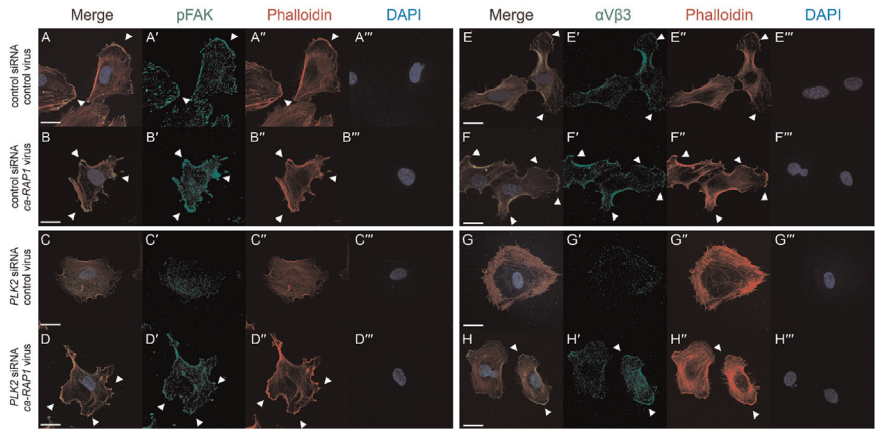

Fig. 6. *PLK2* regulates focal adhesion formation and integrin localization through RAP1 activity. (A–H) Immunofluorescence studies show that *ca-RAP1* virus can rescue the reduced EC sprouting and lamellipodia defects observed in *PLK2* siRNA HUVECs through restoring focal adhesion formation (compare C to D) and integrin αVβ3 organization (compare G to H). Arrowheads point to lamellipodia extension as detected by the organization of F-actin (phalloidin) at the leading edge of extending HUVEC membranes. Green – (A′–D′) anti-pFAK; or (E′–H′) anti-integrin αVβ3; Red – phalloidin; Blue – DAPI. Scale bar, 20 μm.

are long spike-like plasma membrane extensions comprised of tight parallel bundles of filamentous actin (F-actin). On the other hand, lamellipodia are short veil-like structures that are in close proximity to the plasma membrane and exhibit a highly branched actin network (Huber et al., 2003; Mattila and Lappalainen, 2008; Pollard and Borisy, 2003). In many cell types, both cellular processes are able to explore the environment for attractive and repulsive guidance cues (Huber et al., 2003), and form focal adhesions between the cytoskeleton and the ECM to control directional migration (Defilippi et al., 1999). Interestingly, in our knockdown studies, we discovered that *PLK2*-deficient ECs, which exhibit arrested EC sprouting and migration, were able to form filopodia but not lamellipodia, thus suggesting that filopodia may not be sufficient to promote EC sprouting. These results are consistent with those recently reported where ECs treated with low levels of Latrunculin B, which inhibits F-actin polymerization and filopodia formation, were still able to form lamellipodia and sprout, albeit inefficiently (Phng et al., 2013). However, these EC findings are in contrast to studies that report that filopodia may be sufficient to guide neuronal and retinal growth cones (Bentley and Toroian-Raymond, 1986; Chien et al., 1993; Zheng et al., 1996). Although filopodia may not be enough to promote EC sprouting and migration, they may be still required for proper vascular development including efficient EC migration and anastomosis as previously suggested (Phng et al., 2013). Lastly, our data also suggests that lamellipodia may not be required to form filopodia as we did not observe any demonstrable filopodia defects in the *PLK2* knockdown ECs, which exhibited significantly decreased lamellipodia. Thus, future detailed EC cellular studies will be necessary to further examine the specific roles of filopodia and lamellipodia in EC sprouting and migration.

Finally, although Polo-like kinase proteins have been shown to regulate the cell cycle, they may also participate in regulating angiogenesis and vascular development. Here, we showed that *PLK2* is expressed in the vascular system and functions to control vascular development through regulating small GTPases involved in lamellipodia formation of ECs during angiogenesis. Furthermore, PLK3 has been shown to suppress tumor angiogenesis through phosphorylating HIF-1α and PTEN, which destabilizes HIF-1α and stabilizes PTEN, a known regulator of HIF-1α and tumor angiogenesis (Xu et al., 2012, 2010a, 2010b; Yang et al., 2008). Given the biological relationship between angiogenesis, tissue development, and tumor growth, these findings raise the possibility that other PLK family members may also regulate angiogenesis and support further studies to explore their role in vascular development.

Acknowledgments

We thank Neil Tedeschi for expert help with the fish and Mark Ginsberg's lab for ca-RAP1 plasmids. This work was supported in part by grants from the American Heart Association to H.Y. (12POST12050080); and the NIH to N.C.C (HD069305), N.C.C. and J. G.G. (HD070494), T.K.H. (HL111437), and Y.I.M. (HL093767).

Appendix A. Supplementary material

Supplementary data associated with this article can be found in the online version at http://dx.doi.org/10.1016/j.ydbio.2015.05.011.

References

Adams, R.H., Alitalo, K., 2007. Molecular regulation of angiogenesis and lymphangiogenesis. Nat. Rev. Mol. Cell Biol. 8, 464–478.

Bedell, V.M., Yeo, S.Y., Park, K.W., Chung, J., Seth, P., Shivalingappa, V., Zhao, J., Obara, T., Sukhatme, V.P., Drummond, I.A., Li, D.Y., Ramchandran, R., 2005. roundabout4 is essential for angiogenesis in vivo. Proc. Natl. Acad. Sci. USA 102, 6373–6378.

Bentley, D., Toroian-Raymond, A., 1986. Disoriented pathfinding by pioneer neurone growth cones deprived of filopodia by cytochalasin treatment. Nature 323, 712–715.

Bertrand, J.Y., Chi, N.C., Santoso, B., Teng, S., Stainier, D.Y., Traver, D., 2010. Haematopoietic stem cells derive directly from aortic endothelium during development. Nature 464, 108–111.

Bivona, T.G., Quatela, S., Philips, M.R., 2006. Analysis of Ras activation in living cells with GFP-RBD. Methods Enzymol. 407, 128–143.

Brinkmann, T., Daumke, O., Herbrand, U., Kuhlmann, D., Stege, P., Ahmadian, M.R., Wittinghofer, A., 2002. Rap-specific GTPase activating protein follows an alternative mechanism. J. Biol. Chem. 277, 12525–12531.

Carmeliet, P., Tessier-Lavigne, M., 2005. Common mechanisms of nerve and blood vessel wiring. Nature 436, 193–200.

Carmona, G., Gottig, S., Orlandi, A., Scheele, J., Bauerle, T., Jugold, M., Kiessling, F., Henschler, R., Zeiher, A.M., Dimmeler, S., Chavakis, E., 2009. Role of the small GTPase Rap1 for integrin activity regulation in endothelial cells and angiogenesis. Blood 113, 488–497.

Chi, N.C., Shaw, R.M., De Val, S., Kang, G., Jan, L.Y., Black, B.L., Stainier, D.Y., 2008. Foxn4 directly regulates tbx2b expression and atrioventricular canal formation. Genes Dev. 22, 734–739.

Chien, C.B., Rosenthal, D.E., Harris, W.A., Holt, C.E., 1993. Navigational errors made by growth cones without filopodia in the embryonic Xenopus brain. Neuron 11, 237–251.

Chrzanowska-Wodnicka, M., Kraus, A.E., Gale, D., White 2nd, G.C., Vansluys, J., 2008. Defective angiogenesis, endothelial migration, proliferation, and MAPK signaling in Rap1b-deficient mice. Blood 111, 2647–2656.

de Rooij, J., Bos, J.L., 1997. Minimal Ras-binding domain of Raf1 can be used as an activation-specific probe for Ras. Oncogene 14, 623–625.

De Smet, F., Segura, I., De Bock, K., Hohensinner, P.J., Carmeliet, P., 2009. Mechanisms of vessel branching: filopodia on endothelial tip cells lead the way. Arterioscler. Thromb. Vasc. Biol. 29, 639–649.

Defilippi, P., Olivo, C., Venturino, M., Dolce, L., Silengo, L., Tarone, G., 1999. Actin cytoskeleton organization in response to integrin-mediated adhesion. Microsc. Res. Tech. 47, 67–78.

del Toro, R., Prahst, C., Mathivet, T., Siegfried, G., Kaminker, J.S., Larrivee, B., Breant, C., Duarte, A., Takakura, N., Fukamizu, A., Penninger, J., Eichmann, A., 2010. Identification and functional analysis of endothelial tip cell-enriched genes. Blood 116, 4025–4033.

Duncan, P.I., Pollet, N., Niehrs, C., Nigg, E.A., 2001. Cloning and characterization of Plx2 and Plx3, two additional Polo-like kinases from Xenopus laevis. Exp. Cell Res. 270, 78–87.

Gerhardt, H., Golding, M., Fruttiger, M., Ruhrberg, C., Lundkvist, A., Abramsson, A., Jeltsch, M., Mitchell, C., Alitalo, K., Shima, D., Betsholtz, C., 2003. VEGF guides angiogenic sprouting utilizing endothelial tip cell filopodia. J. Cell Biol. 161, 1163–1177.

Hegarty, J.M., Yang, H., Chi, N.C., 2013. UBIAD1-mediated vitamin K2 synthesis is required for vascular endothelial cell survival and development. Development 140, 1713–1719.

Hellstrom, M., Phng, L.K., Hofmann, J.J., Wallgard, E., Coultas, L., Lindblom, P., Alva, J., Nilsson, A.K., Karlsson, L., Gaiano, N., Yoon, K., Rossant, J., Iruela-Arispe, M.L., Kalen, M., Gerhardt, H., Betsholtz, C., 2007. Dll4 signalling through Notch1 regulates formation of tip cells during angiogenesis. Nature 445, 776–780.

Herbert, S.P., Huisken, J., Kim, T.N., Feldman, M.E., Houseman, B.T., Wang, R.A., Shokat, K.M., Stainier, D.Y., 2009. Arterial-venous segregation by selective cell sprouting: an alternative mode of blood vessel formation. Science 326, 294–298.

Huber, A.B., Kolodkin, A.L., Ginty, D.D., Cloutier, J.F., 2003. Signaling at the growth cone: ligand–receptor complexes and the control of axon growth and guidance. Annu. Rev. Neurosci. 26, 509–563.

Jin, S.W., Beis, D., Mitchell, T., Chen, J.N., Stainier, D.Y., 2005. Cellular and molecular analyses of vascular tube and lumen formation in zebrafish. Development 132, 5199–5209.

Kiosses, W.B., Daniels, R.H., Otey, C., Bokoch, G.M., Schwartz, M.A., 1999. A role for p21-activated kinase in endothelial cell migration. J. Cell Biol. 147, 831–844.

Kiosses, W.B., Shattil, S.J., Pampori, N., Schwartz, M.A., 2001. Rac recruits high-affinity integrin alphavbeta3 to lamellipodia in endothelial cell migration. Nat. Cell Biol. 3, 316–320.

Lakshmikanthan, S., Sobczak, M., Chun, C., Henschel, A., Dargatz, J., Ramchandran, R., Chrzanowska-Wodnicka, M., 2011. Rap1 promotes VEGFR2 activation and angiogenesis by a mechanism involving integrin alphavbeta(3). Blood 118, 2015–2026.

Lamalice, L., Le Boeuf, F., Huot, J., 2007. Endothelial cell migration during angiogenesis. Circ. Res. 100, 782–794.

Larrivee, B., Freitas, C., Suchting, S., Brunet, I., Eichmann, A., 2009. Guidance of vascular development: lessons from the nervous system. Circ. Res. 104, 428–441.

Lawson, N.D., Weinstein, B.M., 2002. In vivo imaging of embryonic vascular development using transgenic zebrafish. Dev. Biol. 248, 307–318.

Lee, K.J., Hoe, H.S., Pak, D.T., 2011a. Plk2 Raps up Ras to subdue synapses. Small GTPases 2, 162–166.

Lee, K.J., Lee, Y., Rozeboom, A., Lee, J.Y., Udagawa, N., Hoe, H.S., Pak, D.T., 2011b. Requirement for Plk2 in orchestrated ras and rap signaling, homeostatic structural plasticity, and memory. Neuron 69, 957–973.

Lee, P., Goishi, K., Davidson, A.J., Mannix, R., Zon, L., Klagsbrun, M., 2002. Neuropilin-1 is required for vascular development and is a mediator of VEGF-dependent angiogenesis in zebrafish. Proc. Natl. Acad. Sci. USA 99, 10470–10475.
Lim, J., Choi, H.S., Choi, H.J., 2015. Estrogen receptor-related receptor gamma regulates dopaminergic neuronal phenotype by activating GSK3beta/NFAT signaling in SH-SY5Y cells. J. Neurochem.
Liu, X., Erikson, R.L., 2003. Polo-like kinase 1 in the life and death of cancer cells. Cell Cycle 2, 424–425.
Lowery, D.M., Lim, D., Yaffe, M.B., 2005. Structure and function of Polo-like kinases. Oncogene 24, 248–259.
Lu, X., Le Noble, F., Yuan, L., Jiang, Q., De Lafarge, B., Sugiyama, D., Breant, C., Claes, F., De Smet, F., Thomas, J.L., Autiero, M., Carmeliet, P., Tessier-Lavigne, M., Eichmann, A., 2004. The netrin receptor UNC5B mediates guidance events controlling morphogenesis of the vascular system. Nature 432, 179–186.
Mattila, P.K., Lappalainen, P., 2008. Filopodia: molecular architecture and cellular functions. Nature reviews. Mol. Cell Biol. 9, 446–454.
Mbefo, M.K., Paleologou, K.E., Boucharaba, A., Oueslati, A., Schell, H., Fournier, M., Olschewski, D., Yin, G., Zweckstetter, M., Masliah, E., Kahle, P.J., Hirling, H., Lashuel, H.A., 2010. Phosphorylation of synucleins by members of the Polo-like kinase family. J. Biol. Chem. 285, 2807–2822.
Mukouyama, Y.S., Shin, D., Britsch, S., Taniguchi, M., Anderson, D.J., 2002. Sensory nerves determine the pattern of arterial differentiation and blood vessel branching in the skin. Cell 109, 693–705.
Park, K.W., Morrison, C.M., Sorensen, L.K., Jones, C.A., Rao, Y., Chien, C.B., Wu, J.Y., Urness, L.D., Li, D.Y., 2003. Robo4 is a vascular-specific receptor that inhibits endothelial migration. Dev. Biol. 261, 251–267.
Petrovic, N., Schacke, W., Gahagan, J.R., O'Conor, C.A., Winnicka, B., Conway, R.E., Mina-Osorio, P., Shapiro, L.H., 2007. CD13/APN regulates endothelial invasion and filopodia formation. Blood 110, 142–150.
Phng, L.K., Stanchi, F., Gerhardt, H., 2013. Filopodia are dispensable for endothelial tip cell guidance. Development 140, 4031–4040.
Pollard, T.D., Borisy, G.G., 2003. Cellular motility driven by assembly and disassembly of actin filaments. Cell 112, 453–465.
Roca, C., Adams, R.H., 2007. Regulation of vascular morphogenesis by Notch signaling. Genes Dev. 21, 2511–2524.
Seeburg, D.P., Feliu-Mojer, M., Gaiottino, J., Pak, D.T., Sheng, M., 2008. Critical role of CDK5 and Polo-like kinase 2 in homeostatic synaptic plasticity during elevated activity. Neuron 58, 571–583.
Siekmann, A.F., Lawson, N.D., 2007. Notch signalling limits angiogenic cell behaviour in developing zebrafish arteries. Nature 445, 781–784.
Simmons, D.L., Neel, B.G., Stevens, R., Evett, G., Erikson, R.L., 1992. Identification of an early-growth-response gene encoding a novel putative protein kinase. Mol. Cell. Biol. 12, 4164–4169.
Somanath, P.R., Byzova, T.V., 2009. 14-3-3beta-Rac1-p21 activated kinase signaling regulates Akt1-mediated cytoskeletal organization, lamellipodia formation and fibronectin matrix assembly. J. Cell. Physiol. 218, 394–404.
Spindler, V., Schlegel, N., Waschke, J., 2010. Role of GTPases in control of microvascular permeability. Cardiovasc. Res. 87, 243–253.
Stainier, D.Y., Weinstein, B.M., Detrich 3rd, H.W., Zon, L.I., Fishman, M.C., 1995. Cloche, an early acting zebrafish gene, is required by both the endothelial and hematopoietic lineages. Development 121, 3141–3150.
Steegmaier, M., Hoffmann, M., Baum, A., Lenart, P., Petronczki, M., Krssak, M., Gurtler, U., Garin-Chesa, P., Lieb, S., Quant, J., Grauert, M., Adolf, G.R., Kraut, N., Peters, J.M., Rettig, W.J., 2007. BI 2536, a potent and selective inhibitor of polo-like kinase 1, inhibits tumor growth in vivo. Curr. Biol.: CB 17, 316–322.
Strebhardt, K., 2010. Multifaceted polo-like kinases: drug targets and antitargets for cancer therapy. Nat. Rev. Drug Discov. 9, 643–660.
Suchting, S., Freitas, C., le Noble, F., Benedito, R., Breant, C., Duarte, A., Eichmann, A., 2007. The Notch ligand Delta-like 4 negatively regulates endothelial tip cell formation and vessel branching. Proc. Natl. Acad. Sci. USA 104, 3225–3230.
Torres-Vazquez, J., Gitler, A.D., Fraser, S.D., Berk, J.D., Van, N.P., Fishman, M.C., Childs, S., Epstein, J.A., Weinstein, B.M., 2004. Semaphorin-plexin signaling guides patterning of the developing vasculature. Dev. Cell 7, 117–123.
van Nieuw Amerongen, G.P., Koolwijk, P., Versteilen, A., van Hinsbergh, V.W., 2003. Involvement of RhoA/Rho kinase signaling in VEGF-induced endothelial cell migration and angiogenesis in vitro. Arterioscler. Thromb. Vasc. Biol. 23, 211–217.
Visel, A., Thaller, C., Eichele, G., 2004. GenePaint.org: an atlas of gene expression patterns in the mouse embryo. Nucleic Acids Res. 32, D552–D556.
Warnke, S., Kemmler, S., Hames, R.S., Tsai, H.L., Hoffmann-Rohrer, U., Fry, A.M., Hoffmann, I., 2004. Polo-like kinase-2 is required for centriole duplication in mammalian cells. Curr. Biol.: CB 14, 1200–1207.
Wei, P., Satoh, T., Edamatsu, H., Aiba, A., Setsu, T., Terashima, T., Kitazawa, S., Nakao, K., Yoshikawa, Y., Tamada, M., Kataoka, T., 2007. Defective vascular morphogenesis and mid-gestation embryonic death in mice lacking RA-GEF-1. Biochem. Biophys. Res. Commun. 363, 106–112.
Weitzman, M., Bayley, E.B., Naik, U.P., 2008. Robo4: a guidance receptor that regulates angiogenesis. Cell Adhes. Migr. 2, 220–222.
Wojciak-Stothard, B., Entwistle, A., Garg, R., Ridley, A.J., 1998. Regulation of TNF-alpha-induced reorganization of the actin cytoskeleton and cell-cell junctions by Rho, Rac, and Cdc42 in human endothelial cells. J. Cell. Physiol. 176, 150–165.
Xu, D., Wang, Q., Jiang, Y., Zhang, Y., Vega-Saenzdemiera, E., Osman, I., Dai, W., 2012. Roles of Polo-like kinase 3 in suppressing tumor angiogenesis. Exp. Hematol. Oncol. 1, 5.
Xu, D., Yao, Y., Jiang, X., Lu, L., Dai, W., 2010a. Regulation of PTEN stability and activity by Plk3. J. Biol. Chem. 285, 39935–39942.
Xu, D., Yao, Y., Lu, L., Costa, M., Dai, W., 2010b. Plk3 functions as an essential component of the hypoxia regulatory pathway by direct phosphorylation of HIF-1alpha. J. Biol. Chem. 285, 38944–38950.
Yang, Y., Bai, J., Shen, R., Brown, S.A., Komissarova, E., Huang, Y., Jiang, N., Alberts, G. F., Costa, M., Lu, L., Winkles, J.A., Dai, W., 2008. Polo-like kinase 3 functions as a tumor suppressor and is a negative regulator of hypoxia-inducible factor-1 alpha under hypoxic conditions. Cancer Res. 68, 4077–4085.
Zacchigna, S., Ruiz de Almodovar, C., Carmeliet, P., 2008. Similarities between angiogenesis and neural development: what small animal models can tell us. Curr. Top. Dev. Biol. 80, 1–55.
Zeng, H., Zhao, D., Mukhopadhyay, D., 2002. KDR stimulates endothelial cell migration through heterotrimeric G protein Gq/11-mediated activation of a small GTPase RhoA. J. Biol. Chem. 277, 46791–46798.
Zhang, R., Han, P., Yang, H., Ouyang, K., Lee, D., Lin, Y.F., Ocorr, K., Kang, G., Chen, J., Stainier, D.Y., Yelon, D., Chi, N.C., 2013. In vivo cardiac reprogramming contributes to zebrafish heart regeneration. Nature 498, 497–501.
Zhao, L., Borikova, A.L., Ben-Yair, R., Guner-Ataman, B., MacRae, C.A., Lee, R.T., Burns, C.G., Burns, C.E., 2014. Notch signaling regulates cardiomyocyte proliferation during zebrafish heart regeneration. Proc. Natl. Acad. Sci. USA 111, 1403–1408.
Zheng, J.Q., Wan, J.J., Poo, M.M., 1996. Essential role of filopodia in chemotropic turning of nerve growth cone induced by a glutamate gradient. J. Neurosci.: Off. J. Soc. Neurosci. 16, 1140–1149.
Zhong, H., Xin, S., Zhao, Y., Lu, J., Li, S., Gong, J., Yang, Z., Lin, S., 2010. Genetic approach to evaluate specificity of small molecule drug candidates inhibiting PLK1 using zebrafish. Mol. BioSyst. 6, 1463–1468.